Published in final edited form as:

Eur J Immunol. 2016 April ; 46(4): 897–911. doi:10.1002/eji.201546015.

The Nlrp3 inflammasome, IL-1β, and neutrophil recruitment are required for susceptibility to a non-healing strain of *Leishmania major* in C57BL/6 mice

Melanie Charmoy[1], **Benjamin P. Hurrell**[2], **Audrey Romano**[1], **Sang Hun Lee**[1], **Flavia Ribeiro-Gomes**[1], **Nicolas Riteau**[1], **Katrin Mayer-Barber**[1], **Fabienne Tacchini-Cottier**[2], and **David L. Sacks**[1]

[1]Laboratory of Parasitic Diseases, National Institute of Allergy and Infectious Diseases, National Institutes of Health, Bethesda, Maryland, United States of America [2]Department of Biochemistry, WHO-Immunology Research and Training Center, University of Lausanne, Switzerland

Abstract

Infection of C57BL/6 mice with most *L. major* strains results in a healing lesion and clearance of parasites from the skin. Infection of C57BL/6 mice with the *L. major* Seidman strain (*Lm*Sd) isolated from a patient with chronic lesions, despite eliciting a strong Th1 response, results in a non-healing lesion, poor parasite clearance, and complete destruction of the ear dermis. We show here that in comparison to a healing strain, *Lm*Sd elicited early upregulation of IL-1β mRNA and IL-1β producing dermal cells and prominent neutrophils recruitment to the infected skin. Mice deficient in Nlrp3, ASC, and caspase-1/11, or lacking IL-1β or IL-1 receptor signaling, developed healing lesions and cleared *Lm*Sd from the site. Resistance to *Lm*Sd mice was associated with a stronger antigen-specific Th1 response. The possibility that IL-1β might act through neutrophil recruitment to locally suppress immunity was supported by the healing phenotype observed in neutropenic *Genista* mice. Secretion of mature IL-1β by *Lm*Sd infected macrophages in vitro was dependent on activation of the Nlrp3 inflammasome and caspase-1. These data reveal that Nlrp3 inflammasome dependent IL-1β, associated with localized neutrophil recruitment, plays a crucial role in the development of a non-healing form of cutaneous leishmaniasis in conventionally resistant mice.

Keywords

Leishmaniasis; inflammasome; neutrophils; IL-1β; skin

Corresponding author: David L. Sacks, Laboratory of Parasitic Diseases, NIAID, NIH, Bldg 4, Rm B1-12, 4 Center Dr., MSC 0425, Bethesda, MD 20892, Tel: 301-761-5421, dsacks@nih.gov.

Conflict of Interest: The authors declare no commercial or financial conflict of interest.

Introduction

Leishmania are intracellular kinetoplastid protozoan parasites that produce a wide spectrum of human diseases, ranging from spontaneously healing skin lesions, to more chronic cutaneous or muco-cutaneous lesions and visceral disease that is fatal in the absence of treatment. The murine model of infection with *L. major* has been widely used to understand some of the key immunologic features of human leishmaniasis [1]. In this model, most inbred mouse strains, such as C57BL/6 (B/6), develop a self-healing cutaneous lesion, associated with the development of a polarized $CD4^+$ Th1 response. In contrast, BALB/c mice develop non-healing and disseminating lesions, associated with a predominant Th2 response. Th2 dominance, however, fails to adequately explain the non-healing or reactivation associated pathologies observed in humans with chronic cutaneous or visceral leishmaniasis (VL). Indeed, analysis of chronic localized lesions or VL spleens in humans has revealed increased expression of pro-inflammatory cytokines and high levels of IL-10, but low expression of Th2 cytokines [2, 3].

In this context, we have introduced a model of non-healing *L. major* in conventionally resistant B/6 mice that may better reflect the immunologic conditions associated with chronic forms of leishmaniasis in humans [4]. Using a low dose infection with a strain of *L. major* (*Lm*Sd) isolated from a patient with chronic cutaneous lesions [5], B/6 mice, despite mounting a strong Th1 response, also fail to heal their dermal lesions or to effectively control tissue parasite burden [4]. While elevated production of IL-10 by T cells promotes infection in this model, it does not appear to be a sufficient condition for the evolution of the non-healing phenotype since IL-10 deficient mice or mice treated with anti-IL-10R antibody still have persisting parasites that in the absence of IL-10 regulation produce even more severe pathology in the cutaneous site [4]. Thus other factors are contributing to the non-healing response.

The IL-1 family members are key mediators of inflammatory responses that are made by and act on innate immune and non-hematopoietic cells. They have been implicated in various immunopathologies and autoinflammatory disorders, as well as orchestrating a coordinated immune response against infectious pathogens (reviewed in [6]). The major agonistic proteins in the IL-1 family are IL-1α, IL-1β, and IL-18. While IL-1α is directly active, IL-1β and IL-18 are produced as proforms in the cytosol, and need to be proteolytically processed for their bioactivity. One of the most important enzymes responsible for processing pro-IL-1β and pro-IL-18 into their mature forms is the cysteine protease caspase-1. Caspase-1 is itself produced as an inactive precursor requiring autocatalytic activation that is mediated by large cytosolic protein complexes termed inflammasomes. Inflammasome assembly in most cases occurs when an intracellular sensor molecule is activated and recruits the adapter molecule apoptosis- associated speck-like protein containing a caspase recruitment domain (ASC).

Inflammasome activation and IL-1β production have recently been shown in murine models to be critical for host resistance to infection with diverse *Leishmania* species, including *L. amazonensis, L. braziliensis, and L. infantum* [7]. By contrast, inflammasome activation and IL-1 signaling are dispensable for resistance to *L. major* [7–9], and a recent study revealed

that the Nlrp3 inflammasome actually promoted Th2 development and non-healing lesions due to *L. major* in BALB/c mice [10]. The present study was designed to examine the underlying inflammatory processes that operate in a *L. major* driven Th1 polarized setting to prevent parasite elimination and produce such severe tissue destruction. We identify Nlrp3 inflammasome dependent IL-1β and persistent recruitment of neutrophils to the inflammatory site, as essential components of the non-cure response.

Results

Model of non-healing cutaneous leishmaniasis due to *L. major* in C57BL/6 mice

As previously described [4], mice infected i.d. with 1000 metacyclic promastigotes of the *Lm*Fn strain develop a nodular lesion that spontaneously begins to heal 8–12 weeks post-infection (Fig 1A). In contrast, and as also previously described [4], mice infected i.d. with 1000 metacyclic promastigotes of *Lm*Sd results in development of a non-healing lesion that eventually ulcerates and leads to complete destruction of the ear dermis (Fig 1A). Given the exceptional tissue destruction observed, we added a parameter of pathology based on the following score: 0- no ulcer; 1- ulcer (hole in ear); 2- ear half eroded; 3- ear completely eroded. The mice infected with *Lm*Sd developed lesions that began to ulcerate from wk 12 post-infection, with complete destruction of the ears occurring after 25 wks (Figs 1B & C). Assessment of parasite burdens in the ear and draining lymph node (dLN) (Fig 1D) revealed that *Lm*Sd continued to grow in both sites until wk 12, after which time no significant reduction was achieved (parasite quantification was not carried out on ulcerated ears showing a pathology score of 2 or greater). By contrast, clearance of the *Lm*Fn strain was apparent after 8 wk post-infection in both the ear and dLN. Of note, the *Lm*Sd parasites did not disseminate to other dermal sites and no evidence of visceralization beyond the local dLN was observed (data not shown).

Histologically, the tissue sections revealed a comparable change in the cellularity and architecture of the *Lm*Fn and *Lm*Sd infected ears at 4 and 7 wks post-infection, with a large influx of mononuclear and polymorphonuclear cells into the dermal compartment and evidence of the formation of granulomas in these sites (Fig 2A). Thickening of the epidermal layer was also observed. By 12 wks, the infiltrate in the *Lm*Fn site began to resolve, while the *Lm*Sd site was substantially enlarged and poorly organized. Higher magnification revealed high numbers of parasitized cells at 7 wks in both groups that by 12 wks were almost completely absent in the *Lm*Fn ear, but even more abundant in the *Lm*Sd ear (Fig 2B).

Kinetics and phenotype of inflammatory cell recruitment to the site

In order to better define the events that promote the evolution of the non-cure response following infection with *Lm*Sd, mice were inoculated with 1000 *Lm*Fn or *Lm*Sd metacyclic promastigotes and the sequence of local inflammatory responses at the site of infection was investigated. The myeloid population was identified as $CD11b^+$ cells and further classified based on their expression of Ly6C and Ly6G (Fig 3A), as follows: $Ly6C^{int}$ $Ly6G^+$ (neutrophils); $Ly6C^-Ly6G^-$ (primarily resident dermal macrophages and DCs); $Ly6C^{hi}Ly6G^-$ and $Ly6C^{int}Ly6G^-$ (variable proportions of inflammatory monocytes and

monocyte derived macrophages and DCs). The total number of $CD11b^+$ cells was similarly increased during the first 3 wks of *Lm*Fn and *Lm*Sd infection (Fig 3B). Beginning at 4 wks, there was a dramatic expansion of $CD11b^+$ cells following inoculation of *Lm*Sd that was not observed in the ears of *Lm*Fn infected mice. Neutrophils primarily accounted for the difference in the $CD11b^+$ cell infiltrate at 4 wks, and continued to be recruited in striking numbers throughout the chronic phase in the *Lm*Sd infected ears, whereas they remained a minor population of the inflammatory cells in the *Lm*Fn site. The $Ly6C^{hi}$, $Ly6C^{int}$ and $Ly6C^{neg}$ $CD11b^+$ populations also significantly increased in *Lm*Sd infected ears until week 7, and their total numbers in the site remained greater than the respective populations in the *Lm*Fn infected ears throughout the chronic stage of disease. We also followed the recruitment of $CD4^+$ and $CD8^+$ T cells to the site of infection (Fig 3C). The number of $CD4^+$ T cells present in the site began to increase at 4 wks post-infection in both strains, however, a significantly higher number of $CD4^+$ T cells was observed at all subsequent time points in the *Lm*Sd infected ears, and remained high (approx. 15,000 cells/ear) throughout the chronic phase. $CD8^+$ T started increasing from wk 5 post-infection, and again were found in greater numbers at all subsequent time points in the *Lm*Sd infected ears, stabilized at approx. 5,000 cells/ear during the chronic phase.

Altogether, these data demonstrate that the non-healing infection and severe pathology due to *Lm*Sd is associated with an early and sustained recruitment of neutrophils, $CD4^+$ T cells and $CD8^+$ T cells to the site of infection in the skin.

Non-healing infection is associated with up-regulated early expression of IL-1 in ear dermal cells

The inflammatory infiltrate that preceded and accompanied the development of severe, non-healing lesions in mice infected with *Lm*Sd was associated with significantly elevated mRNA expression in comparison to ear tissue from naïve and *Lm*Fn infected mice for IL-1α and IL-1β, key mediators of the innate response (Fig 4A). Intracellular staining for IL-1α and IL-1β in single cells suspension from 4 wks infected ears showed significantly increased numbers of cells for each cytokine compared to naïve ears, and significantly more IL-1β producing cells were found in *Lm*Sd infected ears compared to *Lm*Fn, (Fig 4B & C). The IL-1β producing cells were confined to roughly equivalent frequencies of $CD11b^+Ly6C^{int}Ly6G^-$ and $CD11b^+Ly6C^-Ly6G^-$ populations (Fig 4D). Neutrophils and $Ly6C^{hi}$ cells were only poorly contributing to IL-1β production. Thus, our data indicate that an early and sustained, localized IL-1 response by innate cells is associated with non-healing lesions in *Lm*Sd infected mice.

In order to better understand the mediators of the inflammatory response to *Lm*Sd, and the early neutrophilic response in particular, expression profiling of additional selected cytokines and chemokines was carried out on ear dermal cells at various times post-infection. As previously described [4], IFNγ mRNA was upregulated early and remained strongly elevated throughout course of infection (Fig S1). IL-17, which can mediate a number of localized, neutrophil associated pathologies, showed a transient spike in transcriptional activity at 5 wks post-infection. CXCL1 mRNA, a known neutrophil chemoattractant, was elevated in the *Lm*Sd infected ears starting at 7 wks, as was IP-10, a

chemokine that plays a role in T cells recruitment. As both IL-10 and IL-27 have been shown to down regulate the IL-17 response during *L. major* infection in B/6 mice [11, 12], mRNA levels for these cytokines were quantified to determine if their expression might be compromised during infection with *Lm*Sd. Expression levels for IL-10 and for the EBI3 chain of the IL-27 heterodimer were elevated as early as wk 3, and remained elevated during the chronic phase. Expression of the IL-27p28 chain was strongly elevated at wks 7 and 12. Furthermore, both IL-10 and IL-27 signaling were shown to be operational during *Lm*Sd infection, since anti-IL-10R treatment of infected B/6 mice, despite reducing the parasite burden in the dLN, resulted in even more severe pathology (Fig S2A), while infection of *IL-27Ra*$^{-/-}$ mice produced the most rapidly destructive dermal pathology that we have observed (Fig S2B). Thus, while infection with *Lm*Sd activates key anti-inflammatory pathways that limit pathology, the IL-10 and IL-27 responses are insufficient to overcome the severe tissue destruction induced by *Lm*Sd.

IL-1β and the Nlrp3 inflammasome are required for non-healing infection

The role of selected up-regulated inflammatory mediators in the non-healing response was investigated using gene knockout mice. Compared to wild type (wt) mice, neither mice deficient in IL-17A (Fig 5A) nor CXCL1 (Fig 5B), showed any alteration in the onset or progression of the lesion, or the development of the severe pathology produced by *Lm*Sd. The *CXCL1*$^{-/-}$ mice showed only a slight reduction in the number of neutrophils present in the chronic lesion (Fig S3), indicating that other neutrophil chemoattractants can mediate the response. By contrast, *IL-1R*$^{-/-}$ mice, deficient in signaling for both IL-1α and IL-1β, began to heal their nodular lesions from 12 wks post-infection without any signs of tissue destruction during 24 wks of observation (Fig 5C). The healing response in the *IL-1R*$^{-/-}$ mice was accompanied by growth of *Lm*Sd in the ear dermis that was comparable to the wt mice during the first 8 wks of infection, followed by effective clearance of parasites from the site (Fig 5C). These findings were extended to mice deficient in the inflammasome components ASC and caspase-1/11, required for inflammasome dependent processing of pro-IL-1β, and in IL-1β itself. In each case, no ulceration following infection with *Lm*Sd was observed, and the dermal lesions were well resolved by the end of the experiment at 28 wks (Fig 5D). The healing response in the *ASC*$^{-/-}$, *caspase-1/11*$^{-/-}$, *IL-1β*$^{-/-}$, and *IL-1R*$^{-/-}$ mice was in each case associated with a significant reduction compared to wt mice in the early influx of CD11b^{+} cells, including neutrophils, to the site (Fig 5E). To determine which NLR might be responsible for promoting the non-healing response, we focused our attention on Nlrp3, since activation of this NLR has been described in response to infection with other *Leishmania* strains [7, 10]. Lesions in *Nlrp3*$^{-/-}$ mice developed identically to wt mice over the first 8 wks of infection, but were completely resolved by 16 wks (Fig 5F), accompanied by an approximate 40 fold reduction in mean parasite load in the ear (Fig 5F).

Together, these data indicate that IL-1β and the Nlrp3 inflammasome play a critical role in promoting persistence of the parasite and development of the severe pathology following infection with *Lm*Sd in B/6 mice.

Cytokine responses associated with enhanced resistance in *IL-1R*$^{-/-}$ and *Nlrp3*$^{-/-}$ mice

We investigated whether IL-1R signaling is modulating the adaptive immune response following *Lm*Sd infection. Antigen-specific cytokine responses in dLN cells at week 9, just prior to the onset of parasite clearance in the IL-1R$^{-/-}$ mice, are shown in Fig. 6A as the frequency of CD4^{+} T cells staining positive for the indicated cytokines, and as the concentration of secreted cytokine detected by ELISA (Fig 6B). Both parameters revealed an increased IFNγ response in the *IL-1R*$^{-/-}$ mice compared to infected wt mice, albeit significant only in the case of secreted IFNγ. By contrast, IL-4 responses were low in both groups, but uniformly lower in the *IL-1R*$^{-/-}$ mice. The upregulation of IL-10 responses was comparable in each group, with a high proportion of the IL-10^{+}CD4^{+} T cells co-expressing IFNγ, as has been previously described [14]. Apart from the extremely low levels of IL-17 detected in the supernatant of antigen-stimulated wt cells, IL-17 responses were undetectable, either as intracellular or released cytokine. Analysis of cytokine production by dLN cells from *Nlrp3−/−* mice revealed a similar trend, with upregulated IFNγ and down-regulated IL-4, though significantly different only in the case of IL-4 (Fig 6C). Analysis of cytokine production by cells recovered from ear lesional tissue at 13–14 wks revealed a highly significant increase in the frequency of IFNγ^{+}CD4^{+} T cells in the IL-1R$^{-/-}$ mice compared to wt mice (Fig 7A), that was associated with a > 10 fold increase in the concentration of secreted cytokine (Fig. 7B). Relative mRNA levels for IL-10 and IL-4 revealed a significant reduction in the expression levels for these cytokines in the ear lesional cells from the IL-1R$^{-/-}$ mice (Fig 7C). Altogether, the data signify a down regulation of antigen-specific IFNγ responses by IL-1R signaling and inflammasome activation following infection with *Lm*Sd in B/6 mice.

Neutropenic *Genista* mice are resistant to *Lm*Sd

The early and sustained recruitment of neutrophils to the site of *Lm*Sd infection in the ear dermis suggested that the neutrophils might themselves contribute to the evolution of the non-cure response. Our attempts to deplete neutrophils from chronic *Lm*Sd lesions using repeated injections of anti-GR-1 antibodies failed to moderate the pathology or to remove neutrophils from the site (Fig S4). So far as we are aware, the sustained antibody-mediated ablation of neutrophil recruitment to sites of chronic inflammation has not been described. The generation of a mutant neutropenic mouse strain on a C57Bl/6 background has been described in which a point mutation in the zinc finger protein Growth Factor Independence 1 (Gfi1) prevents maturation of promyelocyte precursors into mature neutrophils [15]. Infection of *Genista* mice with *Lm*Sd produced nodular lesions that began to be controlled after wk 8 and were substantially resolved by wk 11 (Fig 8A). No ulcerative pathology was observed in the *Genista* mice, in contrast to the wild type mice that developed non-healing lesions with dermal erosion beginning by wk 11. The healing lesions in the *Genista* mice were associated at 11 wks with a significantly reduced number of amastigotes in the ear, though not in the dLN (Fig 8B). The resolving lesions in the *Genista* mice were, as expected, associated with a significantly reduced number of neutrophils in the site (Fig 8C). By contrast, the numbers of CD11b^{+}Ly6C^{hi} and CD11b^{+}Ly6C^{int} cells, as well as CD4^{+} T cells, were not significantly altered compared to wt mice. Importantly, despite the reduced number of neutrophils in the site, the frequency and total number of IL-1β producing cells was not significantly reduced (Fig 8D), consistent with the findings shown in Fig 4C. The data

suggest that the role of neutrophils in promoting infection and pathology is unlikely to be attributed to their providing a major source of IL-1β. Finally, the Th1 response in the *Genista* mice was significantly enhanced already at 5 wks post-infection, as indicated by the increased frequency of IFNγ+CD4+T cells in the dLN (Fig 8E). No significant difference in the response of ear dermal cells was observed at this early time point.

L. major induced IL-1β maturation and caspase-1 activation in vitro

Attempts to detect the active form of IL-1β by western blot analysis of ear dermal cells ex vivo were not successful. We were, however, able to observe the mature 17kDa form of IL-1β by western blot analysis of culture supernatants of infected bone marrow-derived macrophages (BMDMs) in vitro (Fig 9A). The detection of the active form of IL-1β required low dose priming of the infected cells with LPS. Under the conditions of infection and priming used, no difference was observed between the *Lm*Sd and *Lm*Fn strains. Importantly, no processing of pro-IL-1β was observed in culture supernatants of infected BMDMs from Casp1/11$^{-/-}$ mice. Exposure to either *L. major* strain alone upregulated pro-IL-1β observed in the extracts of BMDMs from both the wt and Casp1/11$^{-/-}$ mice. The weaker pro-IL-1β signal in the Casp1/11$^{-/-}$ macrophages is a consistent finding, and may reflect a role for caspase-1 or 11 in the transcriptional regulation of this response, likely via autocrine signaling by the mature, secreted form of IL-1β. While pro-caspase-1 was readily observed in the extracts of the wt cells, the active form of caspase-1 was not detectable either in the extract or supernatant material (data not shown). Western blot analysis of supernatants from LPS treated, *Lm*Sd infected BMDMs from *Nlrp3*$^{-/-}$ mice, confirmed that activation of the Nlrp3 inflammasome was required for secretion of the mature form of IL-1β in vitro (Fig 9B). The release of IL-1β was also assayed by ELISA at different MOIs with *Lm*Sd and showed parasite dose dependent secretion (Fig 9C). No IL-1β was detected in culture supernatants of infected BMDMs from Casp1/11$^{-/-}$ mice, confirming that active caspase-1/11 was required for *L. major* induced IL-1β secretion. The selective caspase-1 inhibitor Z-WEHD-FMK was used to confirm the requirement for caspase-1 activation in the release of IL-1β by *Lm*Sd infected cells in vitro (Fig 8D).

Discussion

We have introduced a physiologic, low dose infection model of non-healing cutaneous leishmaniasis in conventionally resistant C57Bl/6 mice using a strain of *L. major* isolated from a patient with chronic cutaneous lesions [4]. Despite mounting an early and sustained Th1 response and only minimal Th2 or Th17 responses, mice infected with *Lm*Sd fail to efficiently control the infection and develop severe pathology leading to complete destruction of the ear dermis. While IL-10 contributes to the persistence of *L. major* by inhibiting both the magnitude of the Th1 response and the ability of infected macrophages to kill, its elevated expression does not appear to be a sufficient condition for the evolution of the non-healing phenotype since IL-10R blockade enhances parasite clearance accompanied by more severe lesion pathology, and the mice still fail to heal [4, 12]. A recent report described IL-17A as a key mediator of the immunopathology that develops in the absence of IL-10 regulation in B/6 mice infected with a healing strain of *L. major* [12]. The present findings reveal a very different process controlling the non-healing, severe lesion pathology

due to *Lm*Sd, as it occurs both when the IL-10 response is intact and when the IL-17A response is ablated. Importantly, our studies reveal that inflammasome activation and IL-1β are required for the evolution of the non-healing infection and severe pathology due to *Lm*Sd.

The activation of inflammasomes, leading to the maturation and release of the proinflammatory cytokines IL-1β and IL-18, has been shown to promote host defense against a growing list of infectious agents, including *Staphylococcus aureus, Legionella pneumophila, Bacillus anthraxis, Salmonella enterica, Candida albicans*, and influenza virus [16]. Recently, Nlrp3 inflammasome dependent IL-1β was shown to promote resistance to *L. amazonensis* in B/6 mice by inducing NOS2 mediated production of NO [7]. These studies also found that the inflammasome was important for control of in vivo infection with *L. braziliensis* and *L. infantum*, but reported no phenotype when a healing strain of *L. major* was used. Thus, our finding that the Nlrp3 inflammasome - IL-1β axis contributes not to resistance but to a severe susceptibility phenotype in mice infected with *Lm*Sd is so far exceptional as an experimental outcome even within the *Leishmania* genus. Importantly, there is evidence that IL-1β is associated with the severity of cutaneous and visceral disease in humans [17–19].

The contribution of an inflammasome- IL-1β driven process to the severe pathology produced by *Lm*Sd might not be so surprising, especially as neutrophils that are a crucial component of the response, release oxidants and proteases, including matrix metalloproteinases, that can produce extensive bystander tissue damage. We have been careful, however, to also define the susceptibility to *Lm*Sd in terms of the inability to eliminate parasites from the site. In this context, the severe pathology is likely to be secondary to the persistence of the organisms that drive the inflammatory response. Immune compromise by IL-1β would seem paradoxical in this model, especially as it has been shown to induce resistance to other *Leishmania* infections [7] and it operates in the context of a relatively strong *Lm*Sd induced Th1 response [4]. The enhanced resistance to *Lm*Sd observed in the IL-1R$^{-/-}$ mice was nonetheless associated with a substantial upregulation of the Th1 response, as well as further downregulation of the IL-4 response in the lesion and dLN, suggesting that control of *Lm*Sd requires an especially robust and/or more polarized Th1 response. *Lm*Sd is not intrinsically more resistant to IFNγ mediated killing in vitro compared to other *L. major spp.* [4], but it is likely that in vivo the combined action of activating and deactivating cytokines favors the later in *Lm*Sd infection, and that inflammasome dependent IL-1β is a central mediator of this imbalance. IL-1 can compromise Th1 differentiation by decreasing IL-12R expression and by interfering with IL-6-induced phosphorylation of signal transducer and activator of transcription 1 (STAT1) [20, 21]. While we also observed that the low IL-4 response was further attenuated in IL-1R$^{-/-}$ mice, confirming a prior study employing a healing strain of *L. major*[13], IL-1 dependent Th2 expansion is not a sufficient condition for the susceptibility, since IL-4$^{-/-}$ B/6 mice still fail to heal their infections with *Lm*Sd [4]. The ability of the inflammasome to drive susceptibility to *Lm*Sd in B/6 mice thus appears to be different from the recent report describing inflammasome dependent, IL-18 mediated upregulation of IL-4 that promotes susceptibility to *L. major* in BALB/c mice [10].

The possibility that the early and sustained infiltration by neutrophils may compromise the Th1 response and localized pathogen control was addressed by *Lm*Sd infection of *Genista* mice that are severely neutropenic due to a point mutation that prevents maturation of promyelocyte precursors into mature neutrophils [15]. These mice displayed a clear healing phenotype that was associated with a stronger Th1 response, providing direct evidence that neutrophils contribute to the non-cure response. These findings are consistent with a recent report, also employing *Genista* mice, showing reduced pathology, better control of parasites, and enhanced Th1 responses to *L. mexicana* infection [22]. The findings are also consistent with older studies describing a preponderant neutrophilic infiltrate in susceptible BALB/c mice infected with *L. major* [23], and the observation that neutrophil depletion inhibits the early burst of IL-4 and subsequent lesion progression in these mice [24]. A number of mechanisms have been proposed to explain how neutrophils might compromise Th1 development or *Leishmania* killing by innate cells, including their engagement of deactivating receptors on infected macrophages or DCs involved in the clearance of apoptotic cells [25, 26], their release of eicosanoids that dampen the T cell response [27], and as most recently shown in mice infected with *L. mexicana,* their impairment of DCs recruitment to the site of infection [22]. It is also possible that some of the intra-lesional $C11b^{+}Ly6G^{+}$ cells represent a population of immature cells of myeloid origin that function as a subset of myeloid-derived suppressor cells (MDSCs). These cells can be expanded in many pathologic conditions, including chronic infection, to powerfully suppress T cell responses [28].

The association between the healing phenotypes observed in the *IL-1R*$^{-/-}$, *IL-1β*$^{-/-}$, and inflammasome deficient mice and their markedly reduced numbers of early neutrophils recruited to the site indicates that IL-1β is a crucial mediator of the neutrophilic response. The inflammatory functions of IL-1 are well described, including upregulation of primary growth factors, adhesion molecules, and multiple chemokines [6]. It is interesting that CXCL1, an important neutrophil chemoattractant, was not necessary to mediate the IL-1β driven phenotypes, since the *CXCL1*$^{-/-}$ mice failed to heal and still harbored high numbers of neutrophils in their chronic lesions. IL-1β is known to upregulate several neutrophil-active chemokines apart from CXCL1, including CCL4 (MIP-1β) and CXCL2 (MIP-2), as well as lipid mediators, e.g. leukotrienes [29].

In contrast to the striking phenotypes observed using the *Lm*Sd strain, no strong differences in clinical outcome have been observed in either inflammasome deficient or IL-1R deficient B/6 mice infected with a healing strain of *L. major* [7, 8, 13]. Nonetheless, a reduction in tissue parasite burden was reported in *IL-1R*$^{-/-}$ B/6 mice infected with a healing strain [13], and the more severe lesions resulting from anti-IL-10 receptor antibody treatment of B/6 mice infected with a normally healing strain was not observed in infected *IL-1R*$^{-/-}$ mice [12]. Thus, the ability of *Lm*Sd to induce IL-1β in a manner that promotes infection and pathology may not be unique to this *L. major* strain. *Lm*Sd may instead be exceptional amongst *L. major* strains in the early kinetics and/or magnitude of the IL-1β response induced, such that the overall curative response is prevented. The inability to detect a difference in either the pro- or mature forms of IL-1β induced by *Lm*Fn vs. *Lm*Sd in vitro may be related to the nature of the innate cells used and/or the requirement for LPS priming

that may have obscured differences in their intrinsic ability to upregulate IL-1β in the inflammatory setting of the *L. major* loaded dermis.

The more remarkable parasite strain differences are inter-species related, pertaining to the ability of the Nlrp3 inflammasome and IL-1β to promote resistance to *L. amazonensis, L. braziliensis,* and *L. infantum* on the one hand [7], and susceptibility to *Lm*Sd on the other. The underlying explanation for why the Nlrp3 inflammasome-IL-1β axis promotes such disparate clinical outcomes is not understood, but given the accumulating evidence that neutrophils compromise localized immunity, it will be informative to compare the recruitment, activation state, and function of neutrophils in these different inflammatory settings.

In conclusion, our findings extend the role of innate responses involving IL-1β, inflammasome activation, and neutrophil recruitment to the evolution of non-healing infection and severe disease caused by an intracellular pathogen. The findings reveal potentially new targets for immune-based therapies to promote healing of cutaneous leishmaniasis in humans.

Materials and Methods

Mice

C57BL/6 mice were purchased from Taconic Farms. All of the knock-out mice were generated or backcrossed on the C57BL/6 background. IL-1R1 deficient mice [30], obtained through a supply contract between the National Institute of Allergy and Infectious Diseases (NIAID) and Taconic Farms were backcrossed for a minimum of 10 generations. IL-1β deficient mice [30] were originally derived by Y. Iwakura (Tokyo University). ASC deficient mice [31] were backcrossed for more than 9 generations and were originally generated at Millennium Pharmaceuticals, Cambridge, MA. Caspase-1/11 deficient mice were generated as described [32] and subsequently backcrossed for more than 9 generations. The Nlrp3 deficient mice on a pure C57BL/6 genetic background were generated as described [33]. IL-17A deficient animals were generated and provided by Regeneron [34]. CXCL1 deficient animals were kindly provided by Stefanie Vogel (University of Maryland)[35, 36]. IL-27Ra$^{-/-}$ mice, supplied by Genentech, were backcrossed more than 9 generations and were generated as described previously [37]. The characteristics, source and maintenance of *Genista* mice on a pure C57BL/6 genetic background have been previously described [15, 33].

Ethics Statement

All the mice were maintained in the NIAID animal care facility under specific pathogen-free conditions, and used under a study protocol approved by the NIAID animal care and use committee (protocol number LPD 68E). All aspects of the use of animals in this research were monitored for compliance with The Animal Welfare Act, the PHS Policy, the U.S. Government Principles for the Utilization and Care of Vertebrate Animals Used in Testing, Research, and Training, and the NIH Guide for the Care and Use of Laboratory Animals. Animal experimental protocols were approved by the veterinary office regulations of the

State of Vaud, Switzerland, authorization 1266.4-6 to FTC and performed in compliance with Swiss laws for animal protection.

Infection, lesion and pathology measurements

The origin of the *L. major* Seidman (MHOM/SN/74/SD) (*Lm*Sd) and the *L. major* Friedlin V1 (MHOM/IL/80/Friedlin) (*Lm*Fn) strains has been previously described [5, 38]. Promastigotes were grown at 26°C in medium 199 supplemented with 20% heat-inactivated FCS (Gemini Bio-Products), 100 U/ml penicillin, 100 μg/ml streptomycin, 2 mM L-glutamine, 40 mM Hepes, 0.1 mM adenine (in 50 mM Hepes), 5 mg/ml hemin (in 50% triethanolamine) and 1 mg/ml 6-biotin (M199/S). Infective-stage, metacyclic promastigotes were isolated from stationary cultures (5–6 days) by density gradient centrifugation, as described previously [39]. Mice were then inoculated with 1000 metacyclic promastigotes in the ear dermis by intradermal (i.d.) injection in a volume of 10 μl. Lesion development was monitored weekly by measuring the diameter of the ear nodule with a direct-reading Vernier caliper (Thomas Scientific) and pathology was scored using the following scale: 0=no ulcer, 1=ulcer, 2= ear half eroded, 3=ear completely eroded. For histology, ears were fixed at different times post-infection with 4% formaldehyde, cut in 5μm serial sections and stained with hematoxylin and eosin (H&E).

In vivo treatment

IL-10αR mAb (clone1B1.3a) or an isotype control Ab (GL113) was administered i.p. beginning at 12 weeks after infection, with biweekly injections of 0.2 mg mAb/injection for 2 wks. Mice were sacrificed at 14 wks for lesion scoring and parasite enumeration. For neutrophil depletion, mice were treated beginning at 10 weeks after infection, with biweekly i.p. injections of 0.5 mg RB6-8C5 (anti-Gr-1) or GL113 for 2.5 wks. Mice were sacrificed at 12.5 wks and ear tissue processed for parasite enumeration and phenotype analysis of inflammatory cells.

Processing of ear tissues and evaluation of parasite burden

Ear tissue was prepared as previously described [40]. Briefly, the two sheets of infected ear dermis were separated, deposited in DMEM containing 100 U/ml penicillin, 100 μg/ml streptomycin, and 0.2 mg/ml Liberase CI purified enzyme blend (Roche Diagnostics Corp.), and incubated for 1.5 h at 37°C. Digested tissue was processed in a tissue homogenizer (Medimachine; Becton Dickinson) and filtered through a 70 μm cell strainer (Falcon Products). Parasite titrations were performed as previously described [41]. Briefly, tissue homogenates were serially diluted in 96-well flat-bottom microtiter plates containing biphasic medium, prepared using 50 μl NNN medium containing 20% of defibrinated rabbit blood and overlaid with 100 μl M199/S. The number of viable parasites in each ear was determined from the highest dilution at which promastigotes could be grown out after 7–10 days of incubation at 26°C.

In vitro restimulation

For in vitro restimulation of draining lymph nodes cells, 3×10^6 cells were co-cultured with 2×10^6 CD90.2 negative splenic APCs (Miltenyi Biotec) in 1ml of RPMI 1640 containing

10% FCS, 10mM HEPES, glutamine, and penicillin/streptomycin in 48 wells plates with or without 50μg/ml freeze thaw, whole cell killed *Leishmania* Ag prepared from *Lm*Sd stationary-phase promastigotes. After 72h, culture supernatants were collected for ELISA measurements, or cells were stimulated with PMA (10ng/ml) and Ionomycin (500ng/ml) in the presence of Golgistop (BD Biosciences) for 4h before intracellular cytokine staining.

Immunolabeling, flow cytometry analysis, and cytokine measurements

Single-cell suspensions were incubated with an anti-Fc-γIII/II (CD16/32) receptor Ab (2.4G2, BD Biosciences) in PBS containing 1% FCS and stained with fluorochrome-conjugated antibodies for 30 min on ice. The following antibodies were used for surface staining: FITC and PE-anti-mouse Ly6G (1A8, BD Bioscience); PerCP-Cy5.5- anti-mouse Ly6C (HK1.4, eBioscience); PE-Cy7- CD11b (M1/70, eBioscience); PE and PECy7 anti-mouse CD4 (RM4–5, eBioscience); BrillantViolet510- anti-mouse CD4 (RM4–5, Biolgend), APC-eFluor780 anti-mouse CD8 (53-6.7, eBioscience), APC- anti-mouse CD11c (HL3, BD Biosciences), BrillantViolet421 and BrillantViolet450- TCRβ (H57-597, Biolegend). For intracellular detection of cytokines, cells were cultured in the presence of Brefeldin A (1μg/ml, BD Biosciences) and Monensin (5μg/ml, Sigma) for 4h at 37°C. The staining of surface and intracytoplasmic markers was performed sequentially. Cells were first stained for their surface markers, then fixed and permeabilized using BD Cytofix/Cytoperm (BD Biosciences) and finally stained for intracellular detection of cytokines for 30 minutes on ice. The following antibodies were used for cytokine detection: FITC- anti mouse IL-1α (ALF-161, ebioscience), APC- anti mouse IL-1β proform (NJTEN3, ebioscience), FITC-anti-mouse IFN-γ (XMG1.2), PerCp-Cy5.5- anti-mouse IL-17A (eBio17B7), APC- anti-mouse IL-4 (11B11) and PE- anti-mouse IL-10 (JES5-16E3). The isotype controls used (all obtained from eBioscience) were FITC and APC anti-rat IgG1 (eBRG1), PerCp-Cy5.5 anti-rat IgG2a (eBR2a), PE anti-rat (eB149/10H5). The data were collected using FacsDIVA software and a FacsCANTO II flow cytometer (BD Biosciences) and analyzed with FlowJo software (Tree Star). The lymphocytes from ear cells were identified by characteristic size (forward light scatter) and granularity (side light scatter), and by lymphocyte surface phenotype. ELISA measurements for IFNγ, IL-10, IL-4, and IL-17A were performed using eBioscience (San Diego, CA) kits according to manufacture's instructions.

Real time PCR

For analysis of gene expression, ears were processed as described above and single cell suspension immediately placed in RNA lysis buffer (Qiagen). Homogenates were then passed through Qiashredder columns, and RNA was purified using RNAeasy mini kit (Qiagen), according to the manufacturer's protocol. Reverse transcription was performed using Superscript III First-Strand Synthesis System for RT-PCR (Invitrogen Life Technologies). Real-time PCR was performed on an ABI Prism 7900 sequence detection system (Applied Biosystems). PCR primer probe sets were pre-developed gene expression assays designed by Applied Biosystems, and the quantities of products were determined by the comparative threshold cycle method using the equation $2^{-\Delta\Delta Ct}$ (where Ct represents cycle threshold) to determine the fold increase in product. Each gene of interest was normalized to the 18s rRNA endogenous control.

BMDMs generation, infection, and detection of mature and secreted IL-1β

Isolated femurs and tibia were flushed with PBS, and precursor cells were cultured in complete RPMI supplemented with 30% L929 cell-conditioned medium. After 7 d in culture, mature bone marrow-derived macrophages (BMDM) were harvested and infected with metacyclic promastigotes at different multiplicities of infection (MOI). For detection of IL-1β secretion by infected cells by ELISA, BMDMs were primed for 5 h with LPS (50 ng/ml), washed, and then infected with metacyclic promastigotes at different MOIs for 6 hr. Supernatants were assayed using the IL-1β DuoSet ELISA (R&D Systems). For western blot analysis of the active form of IL-1β, BMDMs were treated or not with LPS (50 ng/ml) and infected or not with metacyclic promastigotes at a 1:8 MOI for 6 hr. Supernatants were concentrated by methanol/chloroform precipitation and immunoblotted along with cell extracts for IL-1β (AF-401/R&D) and caspase-1 (M-20/Santa Cruz Biotech). For selective inhibition of caspase-1, BMDMs were pretreated with 20μM and 50 μM of Z-WEHD-FMK or control inhibitor Z-FA-FMK (R&D Systems) for 5 hr prior to infection.

Statistical analysis

Statistical significance between groups was determined by the unpaired, two-tailed student's *t*-test using Prism software (GraphPad).

Supplementary Material

Refer to Web version on PubMed Central for supplementary material.

Acknowledgments

We thank Kim Beacht for assistance with the animal infection studies, and Dragana Jankovic for helpful discussions and provision of the *IL-27Ra*$^{-/-}$ mice, and Marie and Bernard Malissen for the *Genista* mice. This work was supported in part by the Intramural Research Program of the National Institute of Allergy and Infectious Diseases, National Institutes of Health, and in part by the Swiss National Foundation, grant 310030.146187/1 to FTC.

Abbreviations used

VL	visceral leishmaniasis
ASC	apoptosis-associated speck-like protein containing a caspase recruitment domain
dLN	draining lymph node
BMDM	bone-marrow derived macrophages
i.d	intradermal
SN	supernatant
XT	cell lysate

References

1. Sacks D, Noben-Trauth N. The immunology of susceptibility and resistance to Leishmania major in mice. Nature reviews Immunology. 2002; 2:845–858.

2. Louzir H, Melby PC, Ben Salah A, Marrakchi H, Aoun K, Ben Ismail R, Dellagi K. Immunologic determinants of disease evolution in localized cutaneous leishmaniasis due to Leishmania major. The Journal of infectious diseases. 1998; 177:1687–1695. [PubMed: 9607850]

3. Ansari NA, Kumar R, Gautam S, Nylen S, Singh OP, Sundar S, Sacks D. IL-27 and IL-21 are associated with T cell IL-10 responses in human visceral leishmaniasis. Journal of immunology. 186:3977–3985.

4. Anderson CF, Mendez S, Sacks DL. Nonhealing infection despite Th1 polarization produced by a strain of Leishmania major in C57BL/6 mice. Journal of immunology. 2005; 174:2934–2941.

5. Neva FA, Wyler D, Nash T. Cutaneous leishmaniasis--a case with persistent organisms after treatment in presence of normal immune response. Am J Trop Med Hyg. 1979; 28:467–471. [PubMed: 222157]

6. Dinarello CA. Immunological and inflammatory functions of the interleukin-1 family. Annual review of immunology. 2009; 27:519–550.

7. Lima-Junior DS, Costa DL, Carregaro V, Cunha LD, Silva AL, Mineo TW, Gutierrez FR, Bellio M, Bortoluci KR, Flavell RA, Bozza MT, Silva JS, Zamboni DS. Inflammasome-derived IL-1beta production induces nitric oxide-mediated resistance to Leishmania. Nat Med. 2013; 19:909–915. [PubMed: 23749230]

8. Kautz-Neu K, Kostka SL, Dinges S, Iwakura Y, Udey MC, von Stebut E. IL-1 signalling is dispensable for protective immunity in Leishmania-resistant mice. Experimental dermatology. 2011; 20:76–78. [PubMed: 20955202]

9. Satoskar AR, Okano M, Connaughton S, Raisanen-Sokolwski A, David JR, Labow M. Enhanced Th2-like responses in IL-1 type 1 receptor-deficient mice. European journal of immunology. 1998; 28:2066–2074. [PubMed: 9692874]

10. Gurung P, Karki R, Vogel P, Watanabe M, Bix M, Lamkanfi M, Kanneganti TD. An NLRP3 inflammasome-triggered Th2-biased adaptive immune response promotes leishmaniasis. J Clin Invest. 2015

11. Anderson CF, Stumhofer JS, Hunter CA, Sacks D. IL-27 regulates IL-10 and IL-17 from CD4+ cells in nonhealing Leishmania major infection. Journal of immunology. 2009; 183:4619–4627.

12. Gonzalez-Lombana C, Gimblet C, Bacellar O, Oliveira WW, Passos S, Carvalho LP, Goldschmidt M, Carvalho EM, Scott P. IL-17 Mediates Immunopathology in the Absence of IL-10 Following Leishmania major Infection. PLoS pathogens. 2013; 9:e1003243. [PubMed: 23555256]

13. Kostka SL, Knop J, Konur A, Udey MC, von Stebut E. Distinct roles for IL-1 receptor type I signaling in early versus established Leishmania major infections. The Journal of investigative dermatology. 2006; 126:1582–1589. [PubMed: 16645594]

14. Anderson CF, Oukka M, Kuchroo VJ, Sacks D. CD4(+)CD25(−)Foxp3(−) Th1 cells are the source of IL-10-mediated immune suppression in chronic cutaneous leishmaniasis. The Journal of experimental medicine. 2007; 204:285–297. [PubMed: 17283207]

15. Ordonez-Rueda D, Jonsson F, Mancardi DA, Zhao W, Malzac A, Liang Y, Bertosio E, Grenot P, Blanquet V, Sabrautzki S, de Angelis MH, Meresse S, Duprez E, Bruhns P, Malissen B, Malissen M. A hypomorphic mutation in the Gfi1 transcriptional repressor results in a novel form of neutropenia. Eur J Immunol. 2012; 42:2395–2408. [PubMed: 22684987]

16. Franchi L, Munoz-Planillo R, Nunez G. Sensing and reacting to microbes through the inflammasomes. Nat Immunol. 2012; 13:325–332. [PubMed: 22430785]

17. Costa DL, Rocha RL, Carvalho RM, Lima-Neto AS, Harhay MO, Costa CH, Barral-Neto M, Barral AP. Serum cytokines associated with severity and complications of kala-azar. Pathog Glob Health. 2013; 107:78–87. [PubMed: 23683334]

18. Fernandez-Figueroa EA, Rangel-Escareno C, Espinosa-Mateos V, Carrillo-Sanchez K, Salaiza-Suazo N, Carrada-Figueroa G, March-Mifsut S, Becker I. Disease severity in patients infected with Leishmania mexicana relates to IL-1beta. PLoS Negl Trop Dis. 2012; 6:e1533. [PubMed: 22629474]

19. Moravej A, Rasouli M, Kalani M, Asaei S, Kiany S, Najafipour S, Koohpayeh A, Abdollahi A. IL-1beta (−511T/C) gene polymorphism not IL-1beta (+3953T/C) and LT-alpha (+252A/G) gene variants confers susceptibility to visceral leishmaniasis. Mol Biol Rep. 2012; 39:6907–6914. [PubMed: 22311026]

20. Meng G, Zhang F, Fuss I, Kitani A, Strober W. A mutation in the Nlrp3 gene causing inflammasome hyperactivation potentiates Th17 cell-dominant immune responses. Immunity. 2009; 30:860–874. [PubMed: 19501001]
21. Shen X, Tian Z, Holtzman MJ, Gao B. Cross-talk between interleukin 1beta (IL-1beta) and IL-6 signalling pathways: IL-1beta selectively inhibits IL-6-activated signal transducer and activator of transcription factor 1 (STAT1) by a proteasome-dependent mechanism. Biochem J. 2000; 352(Pt 3):913–919. [PubMed: 11104703]
22. Hurrell BP, Schuster S, Grun E, Coutaz M, Williams RA, Held W, Malissen B, Malissen M, Yousefi S, Simon HU, Muller AJ, Tacchini-Cottier F. Rapid Sequestration of Leishmania mexicana by Neutrophils Contributes to the Development of Chronic Lesion. PLoS Pathog. 2015; 11:e1004929. [PubMed: 26020515]
23. Beil WJ, Meinardus-Hager G, Neugebauer DC, Sorg C. Differences in the onset of the inflammatory response to cutaneous leishmaniasis in resistant and susceptible mice. J Leukoc Biol. 1992; 52:135–142. [PubMed: 1506767]
24. Tacchini-Cottier F, Zweifel C, Belkaid Y, Mukankundiye C, Vasei M, Launois P, Milon G, Louis JA. An immunomodulatory function for neutrophils during the induction of a CD4+ Th2 response in BALB/c mice infected with Leishmania major. J Immunol. 2000; 165:2628–2636. [PubMed: 10946291]
25. Laskay T, van Zandbergen G, Solbach W. Neutrophil granulocytes as host cells and transport vehicles for intracellular pathogens: apoptosis as infection-promoting factor. Immunobiology. 2008; 213:183–191. [PubMed: 18406366]
26. Ribeiro-Gomes FL, Peters NC, Debrabant A, Sacks DL. Efficient capture of infected neutrophils by dendritic cells in the skin inhibits the early anti-leishmania response. PLoS pathogens. 2012; 8:e1002536. [PubMed: 22359507]
27. Yang CW, Unanue ER. Neutrophils control the magnitude and spread of the immune response in a thromboxane A2-mediated process. J Exp Med. 2013; 210:375–387. [PubMed: 23337807]
28. Gabrilovich DI, Nagaraj S. Myeloid-derived suppressor cells as regulators of the immune system. Nat Rev Immunol. 2009; 9:162–174. [PubMed: 19197294]
29. Chou RC, Kim ND, Sadik CD, Seung E, Lan Y, Byrne MH, Haribabu B, Iwakura Y, Luster AD. Lipid-cytokine-chemokine cascade drives neutrophil recruitment in a murine model of inflammatory arthritis. Immunity. 2010; 33:266–278. [PubMed: 20727790]
30. Mayer-Barber KD, Andrade BB, Barber DL, Hieny S, Feng CG, Caspar P, Oland S, Gordon S, Sher A. Innate and adaptive interferons suppress IL-1alpha and IL-1beta production by distinct pulmonary myeloid subsets during Mycobacterium tuberculosis infection. Immunity. 2011; 35:1023–1034. [PubMed: 22195750]
31. Sutterwala FS, Ogura Y, Szczepanik M, Lara-Tejero M, Lichtenberger GS, Grant EP, Bertin J, Coyle AJ, Galan JE, Askenase PW, Flavell RA. Critical role for NALP3/CIAS1/Cryopyrin in innate and adaptive immunity through its regulation of caspase-1. Immunity. 2006; 24:317–327. [PubMed: 16546100]
32. Kuida K, Lippke JA, Ku G, Harding MW, Livingston DJ, Su MS, Flavell RA. Altered cytokine export and apoptosis in mice deficient in interleukin-1 beta converting enzyme. Science. 1995; 267:2000–2003. [PubMed: 7535475]
33. Martinon F, Petrilli V, Mayor A, Tardivel A, Tschopp J. Gout-associated uric acid crystals activate the NALP3 inflammasome. Nature. 2006; 440:237–241. [PubMed: 16407889]
34. Leppkes M, Becker C, Ivanov II, Hirth S, Wirtz S, Neufert C, Pouly S, Murphy AJ, Valenzuela DM, Yancopoulos GD, Becher B, Littman DR, Neurath MF. RORgamma-expressing Th17 cells induce murine chronic intestinal inflammation via redundant effects of IL-17A and IL-17F. Gastroenterology. 2009; 136:257–267. [PubMed: 18992745]
35. Boisvert WA, Rose DM, Johnson KA, Fuentes ME, Lira SA, Curtiss LK, Terkeltaub RA. Up-regulated expression of the CXCR2 ligand KC/GRO-alpha in atherosclerotic lesions plays a central role in macrophage accumulation and lesion progression. The American journal of pathology. 2006; 168:1385–1395. [PubMed: 16565511]
36. Shea-Donohue T, Thomas K, Cody MJ, Aiping Z, Detolla LJ, Kopydlowski KM, Fukata M, Lira SA, Vogel SN. Mice deficient in the CXCR2 ligand, CXCL1 (KC/GRO-alpha), exhibit increased

susceptibility to dextran sodium sulfate (DSS)-induced colitis. Innate immunity. 2008; 14:117–124. [PubMed: 18713728]

37. Chen Q, Ghilardi N, Wang H, Baker T, Xie MH, Gurney A, Grewal IS, de Sauvage FJ. Development of Th1-type immune responses requires the type I cytokine receptor TCCR. Nature. 2000; 407:916–920. [PubMed: 11057672]
38. Sacks DL, Barral A, Neva FA. Thermosensitivity patterns of Old vs. New World cutaneous strains of Leishmania growing within mouse peritoneal macrophages in vitro. Am J Trop Med Hyg. 1983; 32:300–304. [PubMed: 6837841]
39. Spath GF, Beverley SM. A lipophosphoglycan-independent method for isolation of infective Leishmania metacyclic promastigotes by density gradient centrifugation. Experimental parasitology. 2001; 99:97–103. [PubMed: 11748963]
40. Belkaid Y, Mendez S, Lira R, Kadambi N, Milon G, Sacks D. A natural model of Leishmania major infection reveals a prolonged “silent” phase of parasite amplification in the skin before the onset of lesion formation and immunity. Journal of immunology. 2000; 165:969–977.
41. Belkaid Y, Kamhawi S, Modi G, Valenzuela J, Noben-Trauth N, Rowton E, Ribeiro J, Sacks DL. Development of a natural model of cutaneous leishmaniasis: powerful effects of vector saliva and saliva preexposure on the long-term outcome of Leishmania major infection in the mouse ear dermis. The Journal of experimental medicine. 1998; 188:1941–1953. [PubMed: 9815271]

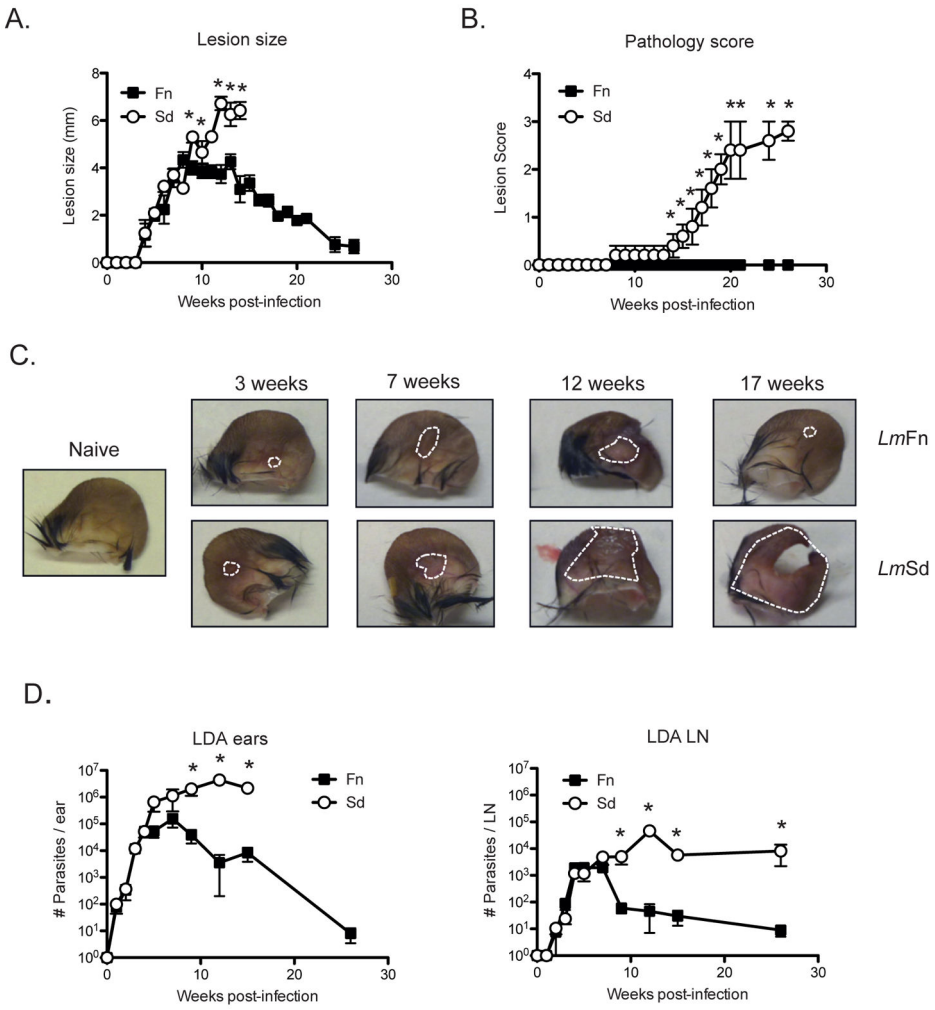

Figure 1. *Lm* Sd produces a non-healing lesion and severe pathology in C57BL/6 mice

C57BL/6 mice were infected in the ear dermis with 1000 *Lm*Fn or *Lm*Sd metacyclic promastigotes. **(A)** Development of nodular lesions and **(B)** pathology score (0=no ulceration, 1=ulcer, 2=half ear eroded, 3=ear completely eroded) over the course of infection. **(C)** Photographs of the ears were taken at different times during the course of infection. Dotted lines circumscribe the nodular lesion. **(D)** Parasite burden as determined by limiting dilution analysis (LDA) in the ear lesion and dLN over the course of infection. Results shown are the mean ± SD of 10 ears, 5 mice/group, * $p<0.05$ comparing infection with *Lm*Fn and *Lm*Sd. The results are representative of at least 3 independent experiments.

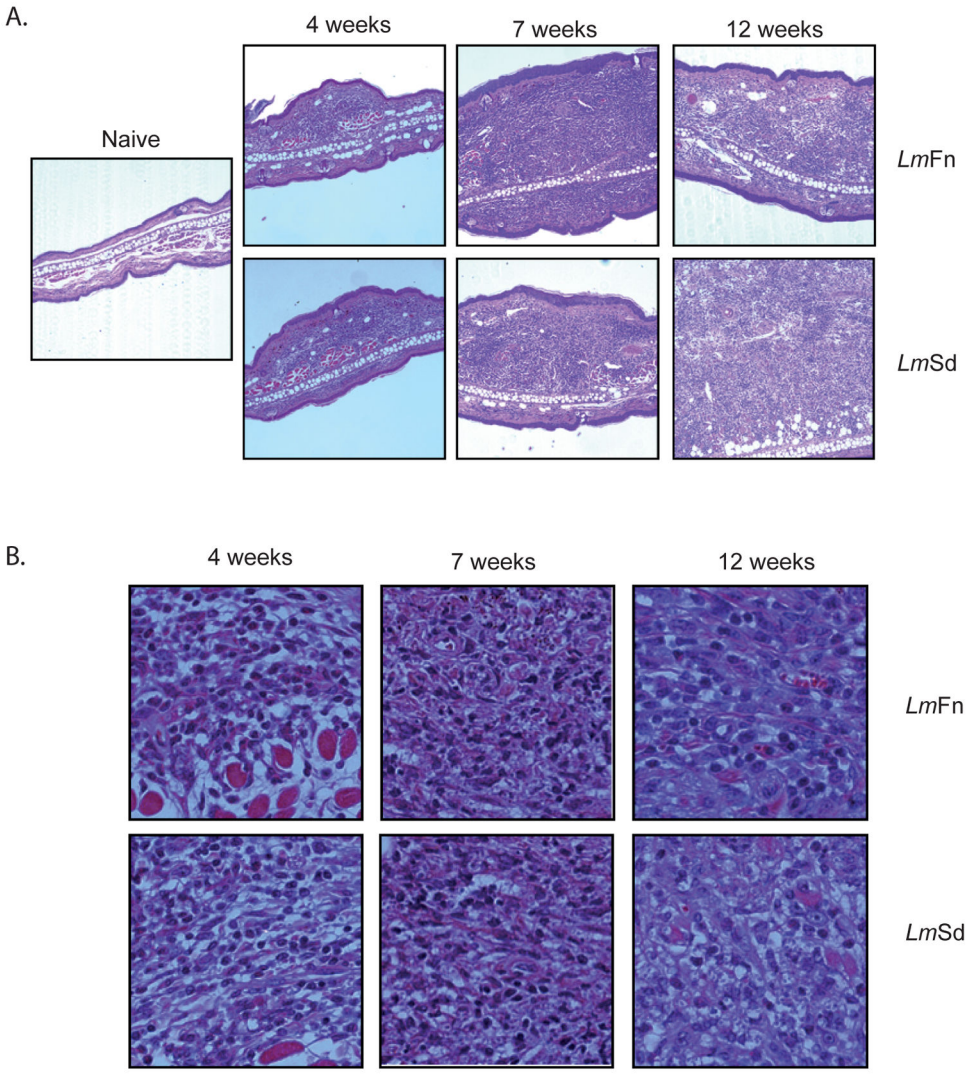

Figure 2. Histopathology of ear lesions

H&E-stained transverse sections of the ears of B/6 mice at various weeks following intradermal inoculation of 1000 *Lm*Fn or *Lm*Sd metacyclic promastigotes. Serial sections through the inoculation site were prepared, and the section showing the greatest transverse thickness at each time point was chosen for presentation. **(E)** Magnification X 100, and **(F)** X 1000; Bar = 10μM.

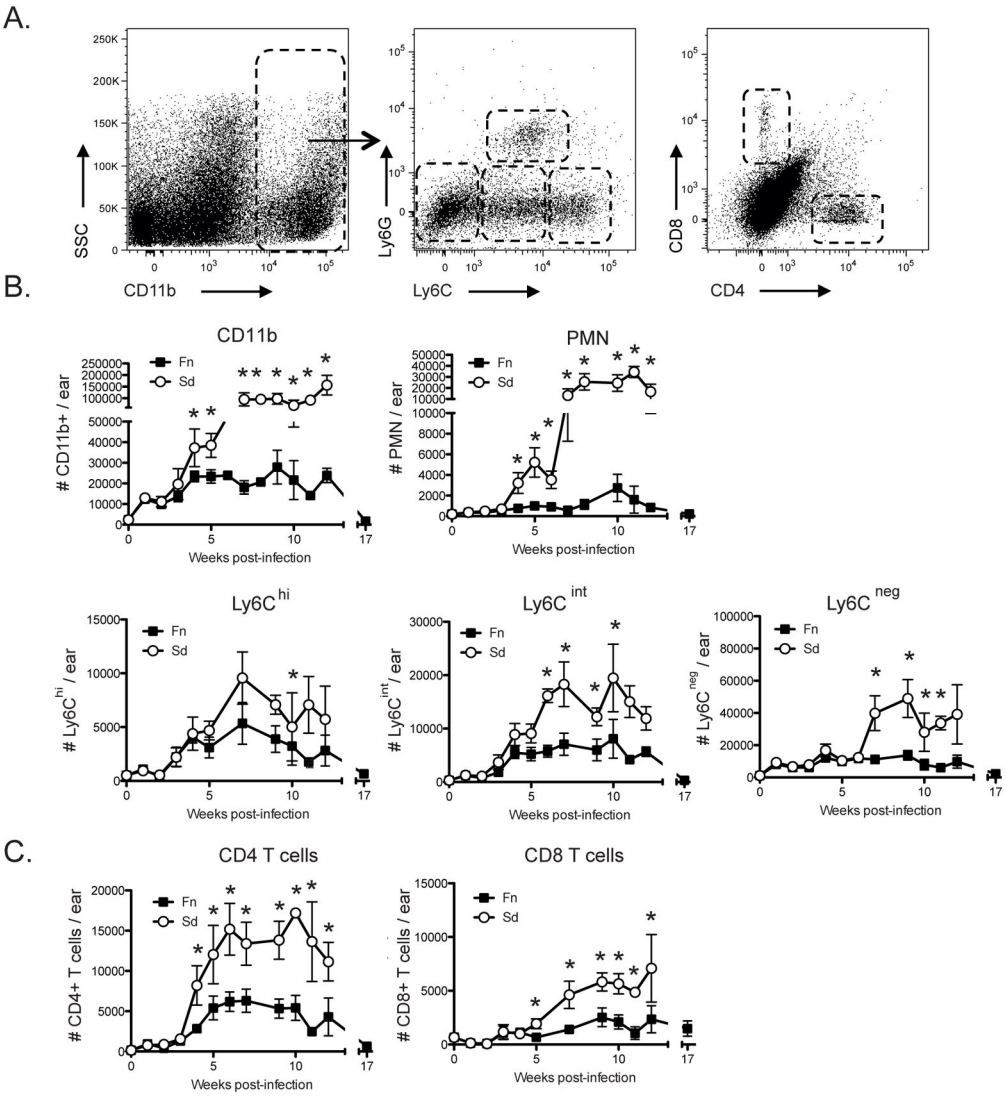

Figure 3. Kinetics of cell recruitment to the site of infection

C57BL/6 mice were infected in the ear dermis with 1000 *Lm*Fn or *Lm*Sd metacyclic promastigotes and ear tissues were processed at different times post-infection to follow the kinetics of cell recruitment. **(A)** Representative dot plots of ear derived dermal cells. Subpopulations of myeloid ($CD11b^+$) cells are defined by the following markers: $Ly6C^{int}$ $Ly6G^+$ (neutrophils); $Ly6C^-Ly6G^-$ (primarily resident dermal macrophages and DCs); $Ly6C^{hi}Ly6G^-$ and $Ly6C^{int}Ly6G^-$ (variable proportions of inflammatory monocytes and monocyte derived macrophages and DCs). T cells were identified by their expression of TCRβ and further separated in $CD4^+$ and $CD8^+$ T cells. **(B)** The number of myeloid cells subsets are represented over the course of infection. **(C)** The number of $CD4^+$ and $CD8^+$ T cells are represented over the course of infection. Values shown are the means ± SD of 8 samples (4 mice, 8 ears) at each time point.

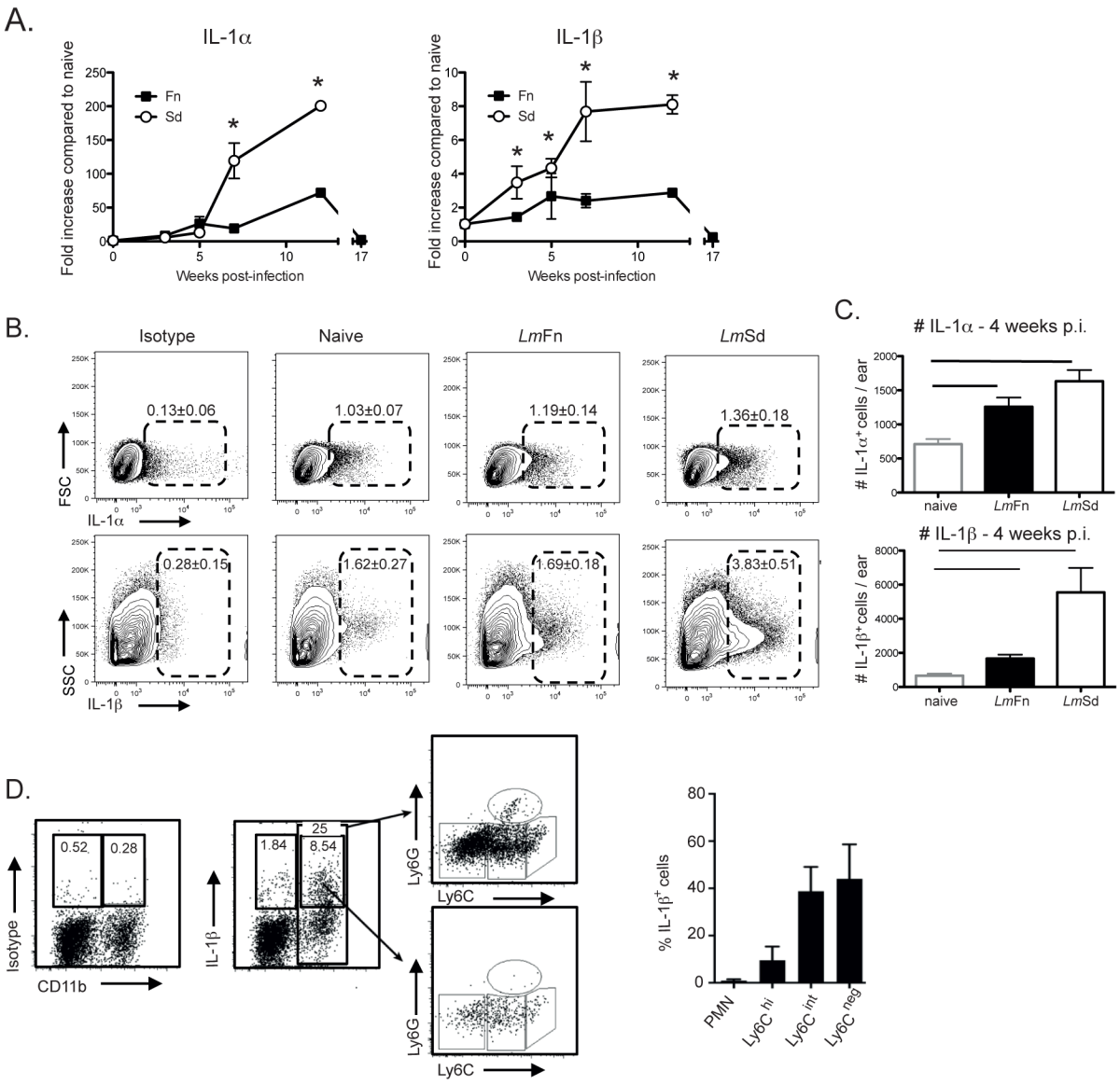

Figure 4. IL-1 expression in ear dermal cells

(A) C57BL/6 mice were infected in the ear dermis with 1000 *Lm*Fn or *Lm*Sd metacyclic promastigotes and total mRNA was isolated from the ear tissue at the indicated times during infection, reverse transcribed and analyzed by real-time PCR for expression of IL-1α and IL-1β. Target genes were normalized to endogenous control, and the values shown are the fold increase relative to expression in naïve ears. Data are represented as means ± SD of 8 samples (4 mice, 8 ears) at each time point. The results are representative of 2 independent experiments. (**B)** Ear tissues were processed for IL-1α and IL-1β intracellular staining at wk 4 post-infection. Representative dot plots are shown. The numbers on the plots represent the percentage of IL-1α and IL-1β positive cells in the ears as a percentage of the total number of viable cells recovered. **(C)** The number IL-1α$^+$ and IL-1β$^+$ cells 4 weeks post infection are represented as means ± SD of 10 ears, 5 mice per group. * $p<0.05$. **(D)** IL-1β intracellular staining at wk 4 post-infection. Shown are the dot plots gated on total CD11b$^+$

cells (top), or CD11b+IL-1β^{+} cells (bottom) and stained for Ly6G and Ly6C. The graph shows the frequency of each subset staining positive for IL-1β as a percentage of the total IL-1β positive cells. Means ± SD, 10 ears, 5 mice.

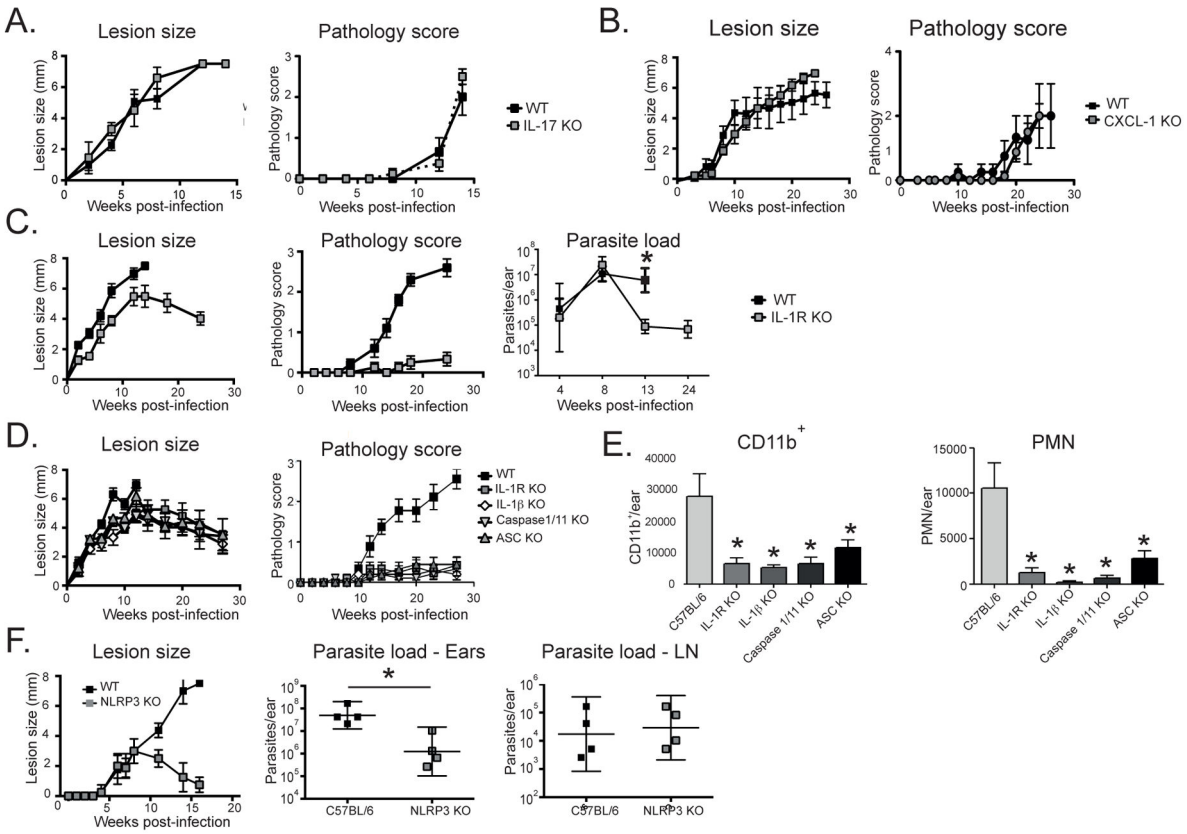

Figure 5. IL-1β and Nlrp3 inflammasome activation are required for non-healing infection and severe pathology due to *Lm*Sd

Lesion development and pathology score over the course of infection with 1000 *Lm*Sd metacyclic promastigotes in the ear dermis in C57BL/6 (WT) and **(A)** *IL-17A*$^{-/-}$, **(B)** *CXCL1*$^{-/-}$, **(C)** *IL-1R*$^{-/-}$, with parasite burden in the ear lesion over the course of infection also shown, **(D)** *IL-1R*$^{-/-}$, *IL-1β*$^{-/-}$, *Caspase1/11*$^{-/-}$ and *ASC*$^{-/-}$ mice, with **(E)** total number of CD11b^{+} and CD11b^{+}Ly6C^{int} Ly6G^{+} (PMN) cells recovered from the ear dermis 4 wks post-infection, and **(F)** *Nlrp3*$^{-/-}$ mice, with parasite burdens in the ear lesion and dLN at 16 wks. Data are means ± SD of 4–10 ears, 4–5 mice per group. * $p<0.05$ comparing lesion size, pathology score, parasite load, or inflammatory cell numbers in WT and KO mice. The results are in each case representative of 2 independent experiments.

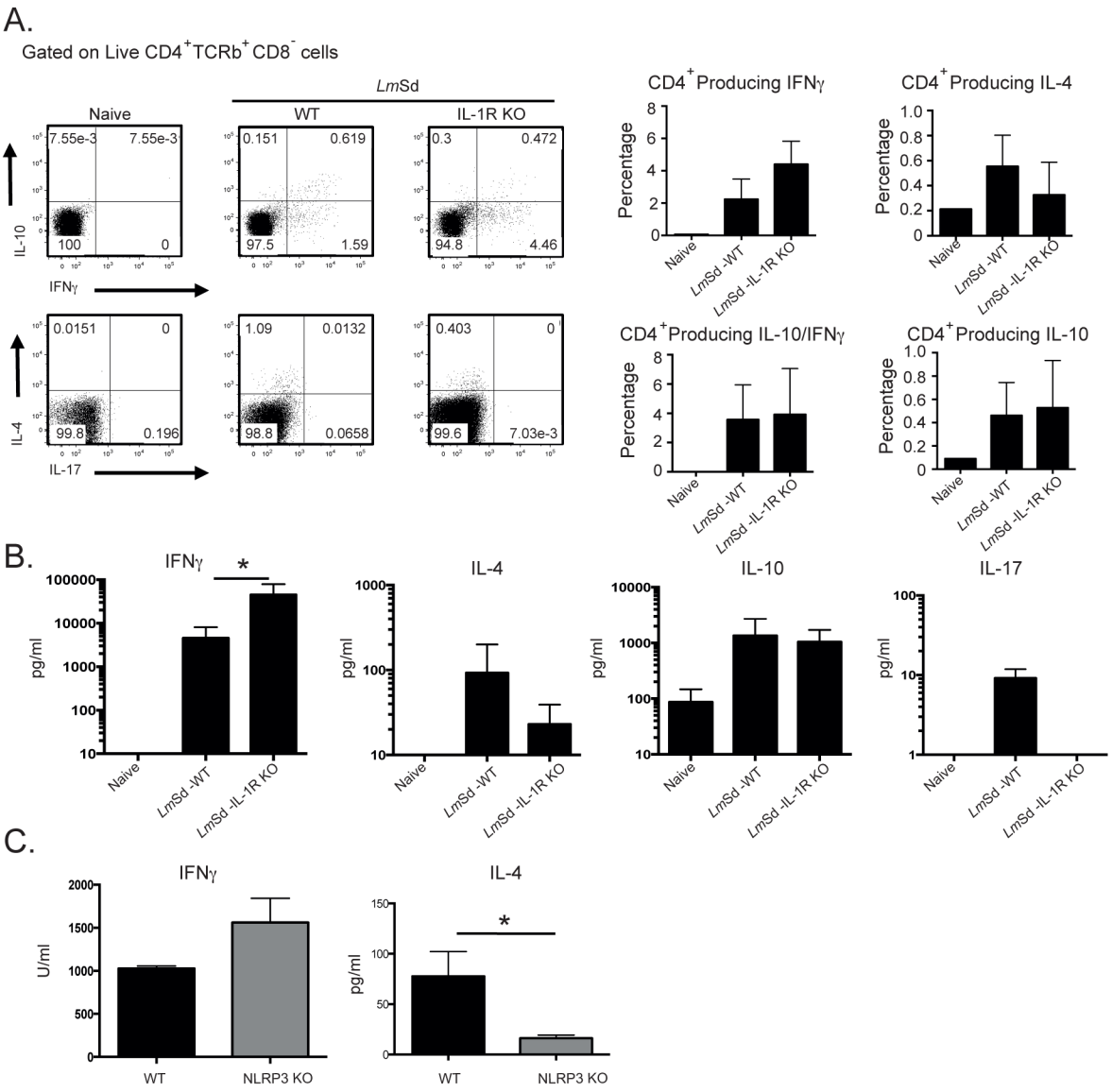

Figure 6. Cytokine responses by dLN cells associated with resistance to *Lm*Sd infection in *IL-1R*$^{-/-}$ and *Nlrp3*$^{-/-}$ mice

C57BL/6 and IL-1R$^{-/-}$ mice were infected in the ear dermis with 1000 *Lm*Sd metacyclic promastigotes. Nine wks post-infection, dLN cells were harvested, stimulated for cytokine production and analyzed by intracellular staining and ELISA. **(A)** Representative dot plots showing the frequency of dLN CD4$^+$ T cells staining positive for selected cytokines following a 4 hr stimulation with PMA/ionomycin. Bar graphs show the frequency of CD4$^+$ T cells staining positive for IFNγ, IL-4, IL-10, or doubly positive for IFNγ and IL-10. IL-17 staining cells were not detected. Data are means ± SD of 3–7 mice per group. **(B)** Concentration of released cytokine in culture supernatants following antigen stimulation of dLN cells recovered from wt and *IL-1R*$^{-/-}$ mice at 9wks, or **(C)** *Nlrp3*$^{-/-}$ mice at 16 wks. Data are means ± SD of 4–8 mice per group; * $p<0.05$.

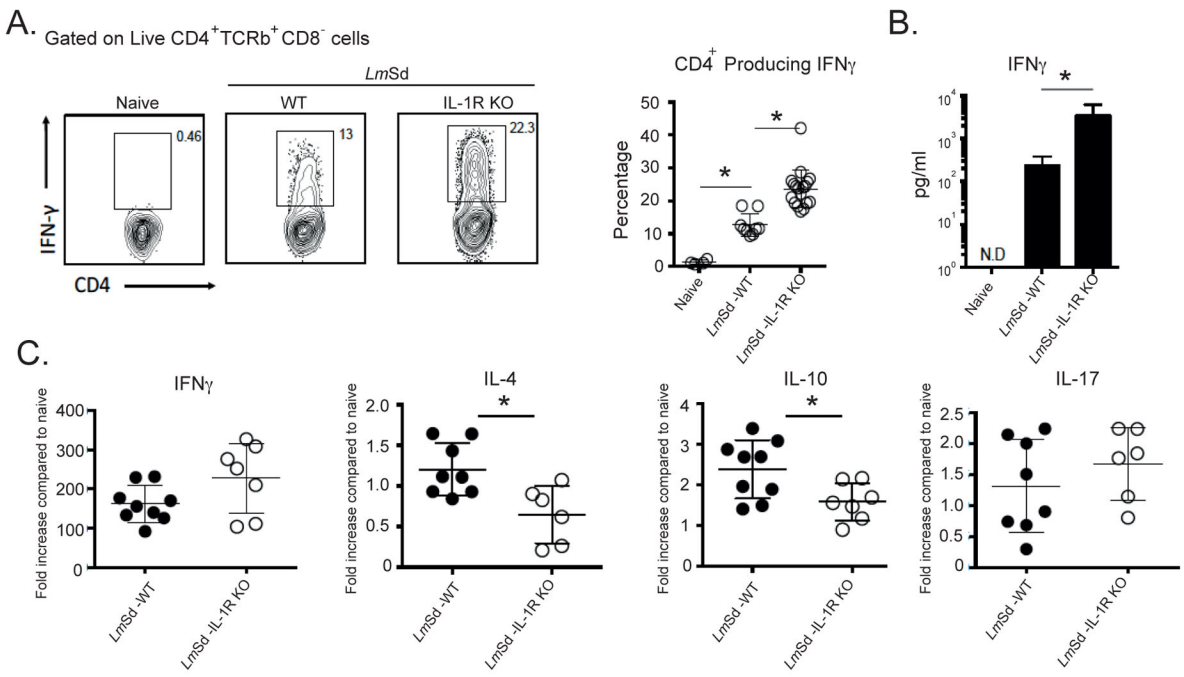

Figure 7. Elevated Th1 response by ear lesional cells associated with resistance to *Lm*Sd infection in *IL-1R*$^{-/-}$ mice

Cells were recovered from the ear dermis at 13 wks post-infection with 1000 *Lm*Sd. (A) Representative dot plots showing the frequency of CD4$^+$ T cells staining positive for IFNγ following a 4 hr stimulation with PMA/ionomycin. Graph shows the frequency of CD4$^+$ T cells present in individual ears staining positive for IFNγ, with means ± SD of the pool of two independent experiments (n=3–5 mice, 6–10 ears/group/experiment); * $p<0.05$. **(B)** Concentration of IFNγ in culture supernatants following Ag stimulation for 72 hr.. Data are means ± SD of 3–7 mice per group; * $p<0.01$. **(C)** Total mRNA was isolated from the ear tissue at 13 wks post-infection, reverse transcribed and analyzed by real-time PCR. Target genes were normalized to endogenous control, and the values shown are the fold increase relative to expression in naïve ears. Data are represented as individual ears with means ± 95% confidence intervals; * $p<0.05$.

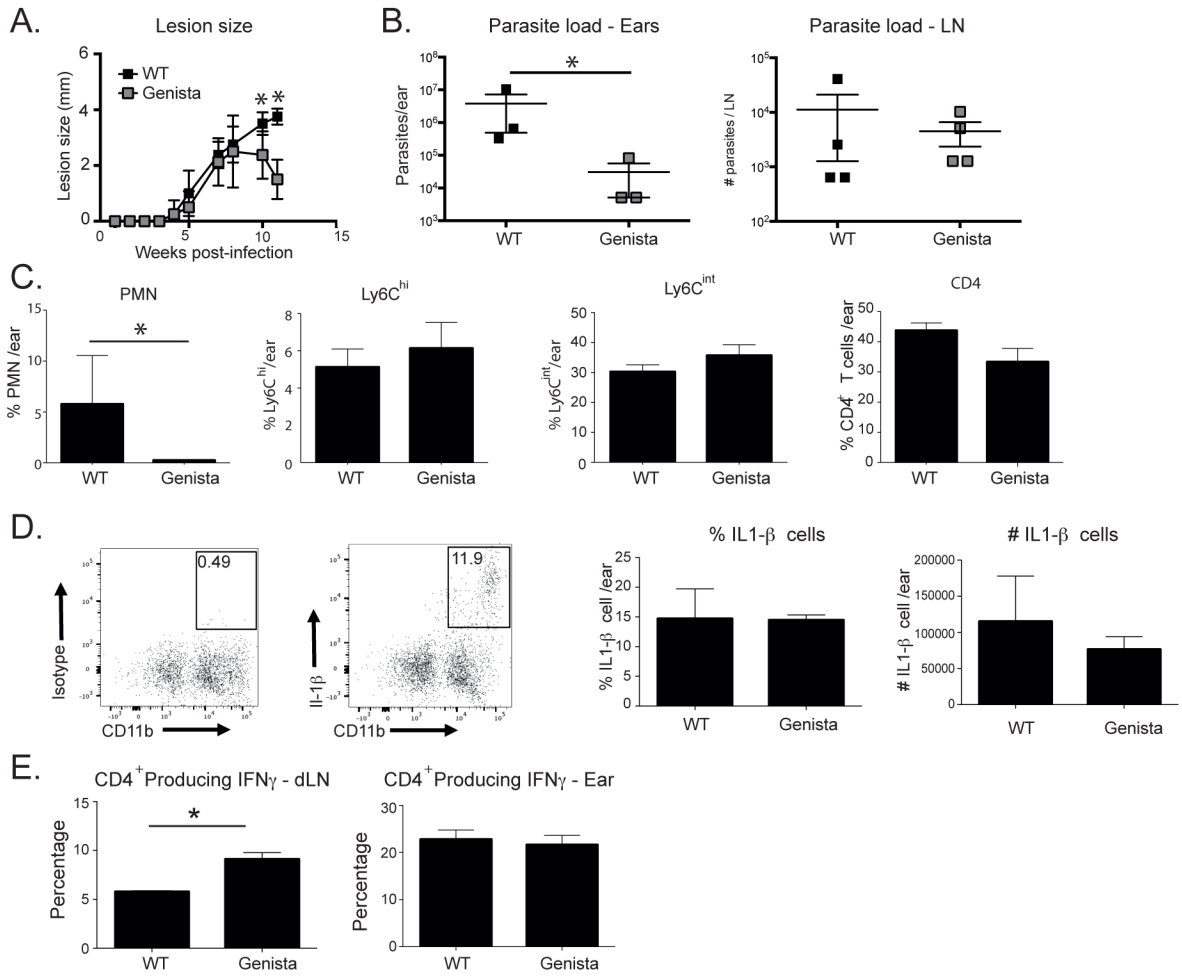

Figure 8. Neutropenic *Genista* mice are resistant to infection with *Lm*Sd

(A) Lesion development in C57Bl/6 and *Genista* mice over the course of infection in the ear dermis with 1000 *Lm*Sd metacyclic promastigotes. Data are means ± SD 4–5 mice per group; * $p<0.05$. One of two representative experiments is shown. **(B)** Parasite burden in the ear lesion and dLN at 11 wks. Results shown are the mean ± SD of 3–4 mice/group; * $p<0.05$. **(C)** Bar graphs show the total number of $CD45^+$ cells and the frequency of myeloid cell subsets and $CD4^+$ T cells recovered from the ear dermis at 5 wks. Data are means ± SD of 3–4 mice per group; * $p<0.05$. One of two representative experiments is shown. **(D)** IL-1β intracellular staining at wk 5, with representative dot plots showing the percentage of IL-IL-1β positive cells in the ears as a percentage of $CD11b^+$ cells. Bar graphs show the frequency and number of IL-$1\beta^+$ cells at 5 wks, represented as means ± SD, 3 mice per group. One of two representative experiments is shown. **(E)** The frequency of $CD4^+$ T cells recovered from dLN or ear at 5 wks post-infection staining positive for IFNγ following a 4 hr stimulation with PMA/ionomycin. Data are means ± SD of 4 mice per group; * $p<0.05$.

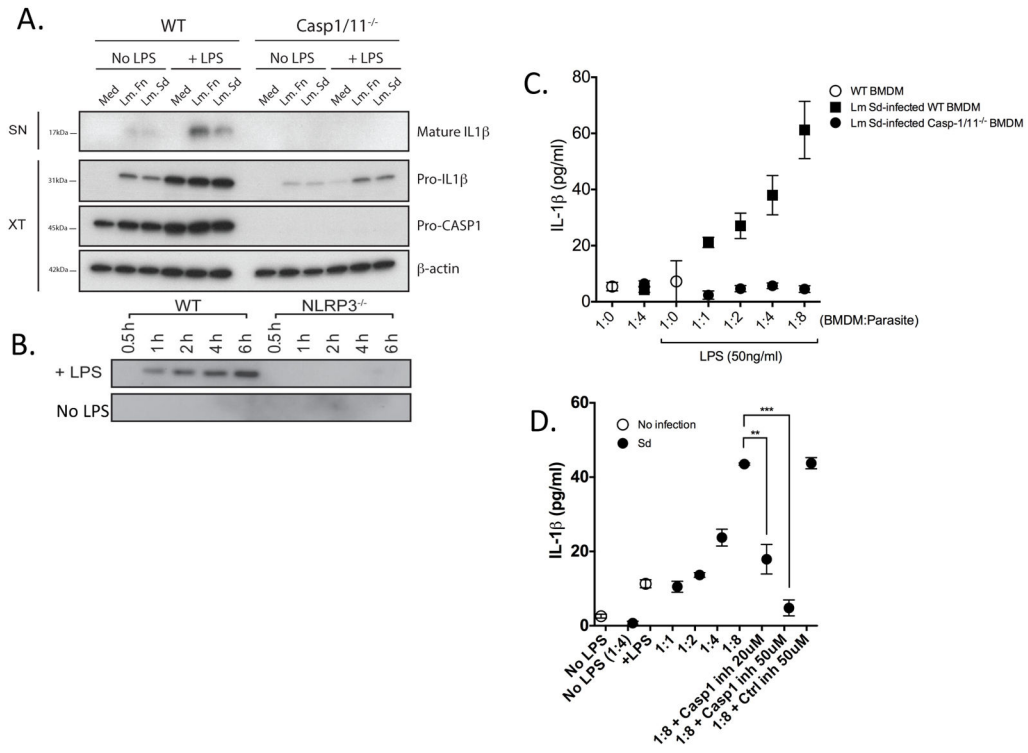

Figure 9. IL-1β release in response to *L. major* infection is dependent on caspase-1 and Nlrp3 inflammasome activation in vitro

(A) Immunoblotting for IL-1β in culture supernatants (SN) from BMDMs prepared from wt or *caspase-1/11*$^{-/-}$ mice treated or not with LPS (50 ng/ml) and infected or not with *Lm*Sd or *Lm*Fn metacyclic promastigotes at an MOI of 1:8 for 6 hr. The cell lysates (XT) were blotted with antibodies against pro-IL-1β, pro-caspase–1, and β–actin. **(B)** Immunoblotting for mature IL-1β in culture supernatants from BMDMs prepared from wt or *Nlrp3*$^{-/-}$ mice treated or not with LPS (50 ng/ml) and infected with *Lm*Sd metacyclic promastigotes at an MOI of 1:8 for 0.5–6 hr. ***(C)*** **(C)** IL-1β concentration in culture supernatants of BMDMs from wt or caspase-1/11$^{-/-}$ mice pre-treated or not with LPS (50 ng/ml) for 5 hrs, followed by infection with *Lm*Sd metacyclic promastigotes at different MOIs for 6 hr. Values shown are means ± SD of quadruplicate assays. **(D)** Conditions of infection and activation of BMDMs are identical to (C), but cells were also pre-treated or not for 5 hr with the selective caspase-1 inhibitor Z-WEHD-FMK or control Z-FA-FMK. ** $p<0.01$; *** $p<0.001$.